JOURNAL OF SOLID STATE CHEMISTRY **65**, 241–250 (1986)

Calorimetric Study of High-Pressure Polymorphs of Li_2WO_4 and Li_2MoO_4

EIJI TAKAYAMA-MUROMACHI

National Institute for Research in Inorganic Materials, Sakura, Niihari, Ibaraki, 305 Japan

ALEXANDRA NAVROTSKY

Dept. of Geological and Geophysical Sciences, Princeton University, Princeton, New Jersey 08544

AND SHINOBU YAMAOKA

National Institute for Research in Inorganic Materials, Sakura, Niihari, Ibaraki, 305 Japan

Received February 10, 1986

Heats of transition among the Li_2WO_4 polymorphs, Li_2WO_4I (phenacite-type structure), Li_2WO_4II, Li_2WO_4III, and Li_2WO_4IV, and that between Li_2MoO_4 (phenacite) and Li_2MoO_4(spinel) were measured by transposed temperature drop calorimetry. The heats of fusion of Li_2WO_4I and Li_2MoO_4(ph) were also obtained. Using these data, the phase boundaries among the polymorphs of Li_2WO_4 and of Li_2MoO_4 were calculated. The calculated phase diagrams were compared with those reported previously. They agree well for Li_2WO_4 but show significant discrepancies, perhaps related to problems in attaining equilibrium at lower temperature, for Li_2MoO_4. © 1986 Academic Press, Inc.

Introduction

Both Li_2WO_4 and Li_2MoO_4 possess phenacite-type structures under some conditions at atmospheric pressure. Their polymorphic behavior, however, is quite different. The phase diagram of Li_2MoO_4 has been reported by Liebertz and Rooymans (*1*). According to them, Li_2MoO_4 undergoes no transition up to its melting point at atmospheric pressure. However, it changes to a polymorph with the normal spinel structure by heating at high pressure. The transition curve was reported to show a negative *dP*/*dT*. The phase diagram of Li_2WO_4 was first reported by Yamaoka *et al.* (*2*), then was reinvestigated by Pistorius (*3*) to clarify liquid and solid boundaries. The phase diagram of Li_2WO_4 is much more complicated than that of Li_2MoO_4. There are four polymorphs including the phenacite type compound, Li_2WO_4I (polymorph notation according to Yamaoka *et al.* (*2*)).

Li_2WO_4II has tetragonal symmetry and the structure is based on cubic close packing of oxygen and is closely related to the β-phase or modified spinel structure of Mg_2SiO_4 (*4*, *5*). Li_2WO_4IV is the densest phase among the four polymorphs. Its structure is based on hexagonal close pack-

0022-4596/86 $3.00
Copyright © 1986 by Academic Press, Inc.
All rights of reproduction in any form reserved.

ing of oxygen, with monoclinic symmetry and is closely related to the wolframite-type structure (*6*, *7*). Li_2WO_4III has orthorhombic symmetry based on hexagonal close packing of oxygen (*8*), but the detailed structure has not been reported.

Subsolidus phase equilibrium studies on Li_2WO_4 and Li_2MoO_4 must be performed at relatively low temperatures where equilibrium states cannot be obtained easily because of the low melting points of the two compounds. An independent method is therefore desirable to confirm the phase diagrams.

In the present work, heats of transition among the polymorphs of Li_2WO_4 and Li_2MoO_4 were determined by means of transposed temperature drop calorimetry (*9*). These data were combined with free energies obtained from phase equilibrium data to calculate the phase boundaries for Li_2WO_4 and Li_2MoO_4. The phase diagrams thus obtained were compared with earlier experimental diagrams.

Experiment

Preparation of samples. Reagent grade Li_2CO_3 and WO_3 were first used as starting materials to make Li_2WO_4I. An equimolar mixture of Li_2CO_3 and WO_3 was fired at ~773 K for ~4 weeks in a Pt crucible with several intermediate grindings. The high-pressure phases were made at the National Institute for Research in Inorganic Materials from the Li_2WO_4I obtained above. The synthesis conditions of each compound are shown in Table I (samples W-1 to W-5). The detailed high-pressure techniques were described elsewhere (*2*). Li_2WO_4IV was prepared in two separate syntheses (W-4 and W-5).

The results of chemical analysis in Table I indicate the ratio, Li/W, is smaller than 2.0 for the samples thus prepared except for Li_2WO_4III (W-3). Moreover, a few small extra peaks were found in the powder X-ray patterns of all these samples. The second phase in the Li_2WO_4I sample was easily identified to be $Li_2W_2O_7$ (*10*), while impurities in the high-pressure samples were difficult to identify. However, after the high-pressure samples were converted to the atmospheric pressure form by annealing at an elevated temperature, we found trace amount of $Li_2W_2O_7$ in them. The content of $Li_2W_2O_7$ was roughly estimated to be ~5 wt% by powder X-ray diffractometry. Since the impurities in the high-pressure samples are unknown phases, it is difficult to make correction for them in the calorimetric data.

TABLE I

PREPARATION OF POLYMORPHS OF Li_2WO_4 AND Li_2MoO_4

Sample	Compound	*P* (GPa)	Conditions *T* (K)	Conditions *t* (hr)	Chemical analysis (Li/W or Li/Mo)
W-1	Li_2WO_4I	1 atm	773	~700	1.9$_4$
W-2	Li_2WO_4II	0.7	773	24	1.8$_7$
W-3	Li_2WO_4III	1.0	923	1	2.0$_4$
W-4	Li_2WO_4IV	4.0	923	2	1.9$_0$
W-5	Li_2WO_4IV	4.0	923	2	1.9$_2$
W-6	Li_2WO_4I	1 atm	823	~500	2.0$_0$
W-7	Li_2WO_4II	1.0	823	48	2.0$_1$
W-8	Li_2WO_4III	1.0	973	16	2.0$_0$
W-9	Li_2WO_4IV	4.0	1013	1	2.0$_5$
M-1	Li_2MoO_4(ph)	1 atm	~773	~700	1.8$_1$
M-2	Li_2MoO_4(sp)	4.0	773	1	1.9$_4$
M-3	Li_2MoO_4(sp)	4.0	773	1	1.9$_0$
M-4	Li_2MoO_4(ph)	1 atm	823	~500	2.0$_6$
M-5	Li_2MoO_4(sp)	by quenching the melt			—

We repeated the synthesis of Li_2WO_4I and the high-pressure polymorphs. This time high-purity-grade Li_2CO_3 (99.99%) and WO_3 (99.9%) were used as starting materials. Moreover, to make Li_2WO_4I a quartz crucible was employed instead of a platinum one to avoid chemical reaction between Li and Pt. The synthesis conditions for the new samples are shown in Table I (W-6 to W-9). The powder X-ray patterns and chemical analysis showed they were single phases.

Thus, we obtained two sets of Li_2WO_4

samples in which the first one contained lithium-poor impurities. We measured calorimetric data for both sets of samples to check the effect on the heats of reaction of small amounts of impurities.

The atmospheric pressure phase of Li_2MoO_4 was also prepared first from the reagent grade Li_2CO_3 and MoO_3 (M-1 in Table I). The spinel-type sample was synthesized twice at 773 K and 4 GPa (M-2 and M-3). Though the results of chemical analysis in Table I shows values of Li/Mo smaller than 2.0, we did not find any impurities by the powder X-ray method. Microscopic observation indicated one of the spinel samples (M-3) contained birefringent crystals showing lower symmetry than the cubic spinel.

We resynthesized Li_2MoO_4(ph) from Li_2CO_3 (99.99%) and MoO_3 (99.9%) using a quartz crucible. The spinel was, at this time, prepared in a different way. We found incidentally that the spinel-type compound could be made even at atmospheric pressure by quenching molten Li_2MoO_4. The Li_2MoO_4(ph) was fired above the melting point in a Pt crucible. Immediately after it was melted completely (to minimize the reaction between Li and Pt), it was quenched by placing the Pt crucible on a metal plate. When the quenching procedure was not proper (due to mechanical shock or insufficient cooling rate), so called "dusting" was observed. Namely, the solidified mass was broken to fine powder owing to the volume expansion caused by spinel to phenacite transition. The sample carefully quenched was identified to be single-phase Li_2MoO_4 (sp) (M-5) by powder X-ray diffraction and microscopic observation. There were no differences either in peak positions or in their relative intensities between the spinel made at high pressure and that made by quenching the melt.

Chemical analysis. Lithium content of each sample was analyzed by means of atomic absorption using a spectrometer (Varian Techtron). Tungsten and molybdenum content were determined by thiocyanate absorptiometry (*11*). In addition, emission spectral analysis was performed to analyze impurity elements using a spectrometer (Shimazu GE-170). The samples made from the reagent grade Li_2CO_3 (W-1 to W-5 and M-1 to M-3) contained ~0.2 wt% Na as the main impurity, while the content of every impurity element was less than 0.02 wt% for the samples made from high-purity-grade Li_2CO_3.

Transposed temperature drop calorimetry. Preliminary experiments revealed that every high pressure polymorph of Li_2WO_4 and Li_2MoO_4 can be converted to the phenacite form within several minutes by annealing at 873° for the tungstate and 773°C for the molybdate. Thus the enthalpy of transformation can be determined directly by dropping the sample from room temperature into a calorimeter at the appropriate high temperature and then repeating the experiment on the transformed sample. The difference between these two measurements gives the enthalpy of transformation at room temperature. This method (transposed temperature drop calorimetry) has been described elsewhere (*9*).

About 30 mg of Li_2MoO_4 or Li_2WO_4 sample were placed in a small Pt capsule made of thin Pt foil (0.0005 in. thickness). The weight of the capsule was about 6 mg. Before dropping into the calorimeter, the sample was dried at 423 K for 2 hr with no observable loss in weight, then the upper part of the capsule was closed tightly and the capsule was shaped to approximate a sphere with diameter of ~5 mm. The calorimeter used was a commercially available Setaram "HT-1500°C" type, which consists of small sample and reference chambers connected by crowns of thermopiles. It is a heat flow calorimeter characterized by high sensitivity and rapid response time. The calorimeter was filled by Ar gas at atmospheric pressure and temperature was maintained at 873° ± 1 K for the Li_2WO_4 sample and at 773 ± 1 K for Li_2MoO_4. In addition, Li_2WO_4I and Li_2MoO_4(ph) were dropped into the calorimeter maintained at various temperatures near their melting points to obtain heats of fusion. The weight of the specimen was checked before and after dropping. It showed no significant change. Each high-pressure sample was dropped twice. If the transformation to phenacite form occurs completely at the first drop, the enthalpy of the second drop corresponds to the heat content of the phenacite-type compound.

Dried reagent grade alumina (corundum) was used to measure the calibration factor of the calorimeter. About 30 mg of alumina was wrapped with Pt foil in the same way as Li_2WO_4 or Li_2MoO_4 and dropped into the calorimeter. Calibration runs and sample runs were alternated. The calibration factor was calculated from the known weight of alumina and platinum using the heat content of alumina (*12*) and platinum (*13*) previously reported.

Results and Discussion

Heat of Transition

In Table II, apparent heat contents of Li_2WO_4 and Li_2MoO_4 polymorphs are shown. As described before, the first set of

TABLE II

APPARENT HEAT CONTENT OF Li_2WO_4 AND Li_2MoO_4 POLYMORPHS DETERMINED BY TRANSPOSED TEMPERATURE DROP CALORIMETRY

		$H^\circ_T - H^\circ_{298}$ (kJ/mole)		
Sample[a]	Compound	First drop	Second drop	T (K)
W-1	Li_2WO_4I	90.53 ± 1.79 (6)[b,c]		873
W-2	Li_2WO_4II	103.90 ± 2.38 (9)	93.80 ± 2.32 (9)	873
W-3	Li_2WO_4III	94.31 ± 1.03 (5)	91.39 ± 2.05 (5)	873
W-4	Li_2WO_4IV	99.17 ± 1.38 (5)	90.99 ± 1.29 (5)	873
W-5	Li_2WO_4IV	101.51 ± 1.90 (5)	89.47 ± 1.77 (5)	873
W-6	Li_2WO_4I	93.48 ± 1.47 (13)		873
W-7	Li_2WO_4II	103.16 ± 1.53 (6)	92.78 ± 1.00 (3)	873
W-8	Li_2WO_4III	94.36 ± 2.31 (6)	92.96 ± 3.03 (3)	873
W-9	Li_2WO_4IV	100.99 ± 1.28 (6)	93.10 ± 0.84 (3)	873
W-6	Li_2WO_4I	120.32 ± 4.49 (3)		1006
W-6	Li_2WO_4I	120.89 ± 2.02 (3)		1010
W-6	Li_2WO_4I	167.54 ± 0.39 (3)		1016
W-6	Li_2WO_4I	126.79 ± 2.83 (3)		1019
M-2	Li_2MoO_4(sp)	74.41 ± 1.03 (6)	74.74 ± 0.51 (6)	773
M-3	Li_2MoO_4(sp)	78.33 ± 1.09 (6)	78.04 ± 0.49 (3)	773
M-4	Li_2MoO_4(ph)	76.05 ± 1.03 (9)		773
M-5	Li_2MoO_4(sp)	73.97 ± 1.13 (6)	76.42 ± 1.87 (6)	773
M-4	Li_2MoO_4(ph)	117.05 ± 3.49 (3)		963
M-4	Li_2MoO_4(ph)	113.40 ± 1.26 (3)		968
M-4	Li_2MoO_4(ph)	140.04 ± 3.06 (3)		973
M-4	Li_2MoO_4(ph)	161.99 ± 3.56 (3)		977
M-4	Li_2MoO_4(ph)	162.04 ± 5.34 (3)		982
M-4	Li_2MoO_4(ph)	166.90 ± 5.06 (3)		988

[a] The sample number in this table corresponds to that in Table I.

[b] Error is standard deviation.

[c] The number in parentheses is the number of calorimetric experiments.

Li_2WO_4 samples (W-1 to W-5) contain a lithium-poor impurity. However, values of the enthalpy seen in the first drop of the high-pressure polymorph are very similar for the first and second set of samples, suggesting that the impurity did not seriously affect the result. The value obtained from the second drop experiment is in good agreement with that for Li_2WO_4I for each set of samples. This is consistent with complete transition from the high-pressure form to the phenacite structure during the first drop experiment. The heat content of Li_2WO_4I from sample (W-1) is a little smaller than that from sample (W-6). Though the difference is not statistically significant, it could be related to the $Li_2W_2O_7$ contained in the sample (W-1). We actually prepared $Li_2W_2O_7$ and measured its heat content ($H^\circ_{873} - H^\circ_{298}$). The result was 283.6 ± 1.5 J/g which is smaller than 357.1 J/g of Li_2WO_4I. Thus this impurity would affect the heat content in the observed direction.

To obtain the heat of fusion of Li_2WO_4I, drop runs were performed at four calorimeter temperatures. The apparent heat content changed sharply between 1010 and 1016 K, consistent with the melting point (1013 K) previously reported (*3*).

As the heat content of Li_2WO_4I, we adopted the average among the value for impurity-free Li_2WO_4I and the second drop data of the polymorphs (W-7 to W-9). The resulting value is 93.26 ± 1.53 kJ/mole. As the apparent heat content of Li_2WO_4II, III, and IV, the first drop values of the impurity-free polymorph (W-7, W-8, and W-9) were used, respectively. For the heat of fusion of Li_2WO_4I, we took the value of $[H^\circ_{1016} - H^\circ_{1010}]$ which is 46.64 ± 7.05 kJ/mole.

There is a difference of about 4 kJ/mole between the apparent heat content of two batches of Li_2MoO_4(sp) made at high pressure. As described before, one of them (M-3) contained birefringent crystals. The enthalpy difference may be caused by the impurity. The first drop value of the other high-pressure spinel sample is in good agreement with that of the sample prepared by the quenching method (M-5). The second drop value of the Li_2MoO_4(sp) is in good agreement with that of Li_2MoO_4(ph).

To get the heat of fusion of Li_2MoO_4(ph), it was dropped into the calorimeter fixed at six different temperatures. The apparent heat content changed greatly between 968 and 977 K, while it had an intermediate value at 973 K. This suggests the melting point of Li_2MoO_4(ph) is ~973 K, supporting the earlier value (978 K) (*1*).

In the first drop data of Li_2MoO_4(sp), one datum (M-3) was omitted and other two data (M-2 and M-5) were averaged to get the apparent heat content of Li_2MoO_4(sp) (74.19 ± 1.05 kJ/mole). The second drop values (except for M-3) and the value of Li_2MoO_4(ph) were averaged to obtain 75.78 ± 1.36 kJ/mole as the heat content of Li_2MoO_4(ph). As the heat of fusion of Li_2MoO_4(ph), we used the value of $[H^\circ_{977} - H^\circ_{968}]$ (48.59 ± 3.78 kJ/mole).

Using these heat content data, heats of transition among the polymorphs of Li_2WO_4 and Li_2MoO_4 were calculated and are shown in Table III.

Phase Diagram of Li_2WO_4

Using the present heat of transition, the phase boundary is calculated by the thermodynamic equation

$$\Delta G_{T,P} = \Delta H^\circ_T - T\Delta S^\circ_T + \int_{1\ \mathrm{atm}}^{P} \Delta V_{T,P}\, dP = 0. \quad (1)$$

Neglecting the thermal expansion, compressibility, and the temperature dependence of ΔH° and ΔS° (since these are unknown for the present compounds), we get

$$\Delta H^\circ - T\,\Delta S^\circ + P\,\Delta V^\circ = 0. \quad (2)$$

One can calculate the ΔS° for given ΔH°

TABLE III

THERMOCHEMICAL DATA FOR TRANSITIONS IN Li_2WO_4 AND Li_2MoO_4

Transition	ΔV°_{298} (cm^3/mole)	ΔH°_{298} (J/mole)	ΔS° (J/mol K^{-1})	dP/dT (GPa/K)
Li_2WO_4				
II → I	12.11[a]	9903 ± 2171[l]	14.8 ± 2.5[l,m]	(0.123 ± 0.020) × 10^{-2}[l,m]
III → I	12.49[b]	1096 ± 2782	4.9 ± 2.7	(0.392 ± 0.219) × 10^{-3}
III → II	0.38[c]	−8807 ± 2782	−10.0 ± 3.3	−0.0262 ± 0.0088
IV → II	1.67[d]	−2180 ± 1996	0.1 ± 2.6	(0.57 ± 0.15) × 10^{-4}
IV → III	1.29[e]	6627 ± 2644	10.0 ± 3.1	(0.78 ± 0.24) × 10^{-2}
I → liq	0.45[f]	46643 ± 2054[n]	46.0 ± 2.0[n]	
	0.4[g]		40[g]	0.103[g]
III → liq	12.94[h]	47739 ± 3460[h]	50.9 ± 3.4[h]	0.00394[h]
	13[g]		40[g]	0.0032[g]
Li_2MoO_4				
sp → ph	11.95[i]	−1590 ± 1715	3.2 ± 2.7	(0.265 ± 0.228) × 10^{-3}
ph → liq	0.45[j]	48588 ± 3782[o]	49.7 ± 3.90[o]	0.110
sp → liq	12.40[k]	46999 ± 4155[k]	52.8 ± 4.7[k]	0.0043[k]

[a] From Refs. (*4, 14*).

[b] From Refs. (*8, 14*).

[c] From Refs. (*4, 8*).

[d] From Refs. (*4, 6*).

[e] From Refs. (*6, 8*).

[f] Calculated in the present work (see text).

[g] After Pistorius (*3*).

[h] Calculated from the value of the transition of I/liq and I/III.

[i] From Refs. (*1, 15*).

[j] Estimated.

[k] Calculated from the value of the transition of ph/liq and sp/ph.

[l] Error is standard deviation.

[m] Error in ΔS° and dP/dT does not include the uncertainty of equilibrium P,T point.

[n] Value at 1013 K.

[o] Value at 978 K.

and ΔV°, if one equilibrium P,T point is known. Then the phase boundary is obtained from the Clausius-Clapeyron equation,

$$dP/dT = \Delta S/\Delta V. \qquad (3)$$

To choose an equilibrium point, we selected a pressure and temperature where the reaction had been reversed rather than a synthesis point. Yamaoka *et al.* (*2*) did three reversal experiments near the phase boundary of Li_2WO_4II and Li_2WO_4IV. Adopting two runs at higher temperatures, 793 K, 1.4 GPa (II → IV) and 773 K, 1.3 GPa (IV → II), an average equilibrium point was decided to be 783 K, 1.35 GPa. The ΔS° (II → IV) and the dP/dT calculated from this point are both close to zero, and the phase boundary is, therefore, nearly independent of temperature as shown in Table III and Fig. 1.

Using two reversal runs by Yamaoka *et al.*, 883 K, 1.55 GPa (IV → III) and 853 K, 1.7 GPa (III → IV), the equilibrium III/IV was estimated as 868 K, 1.62 GPa. The phase boundary calculated from this point and the thermochemical data is very close to that found by Yamaoka *et al.* There are no useful reversal runs in the phase equilibrium study by Yamaoka *et al.* to decide the II/III phase boundary. From the present phase boundaries of II/IV and III/IV, the triple point II/III/IV is 833 K, 1.35 GPa which agrees well with that found by Yamaoka *et al.* (818 K, 1.3 GPa). Based on the present triple point, the II/III boundary was calculated as shown in Table III and Fig. 1. The thermochemical boundary is significantly different from the experimental one. However, the present boundary is not necessarily in conflict with the phase equilibrium runs by Yamaoka *et al.* if the II/III reaction is sluggish. This assumption may be reasonable considering the small volume change between II and III (0.38 cc/mole).

Pistorius (*3*) determined the triple point of I/III/liq by means of high-pressure DTA. Using his value (1016 K, 0.31 GPa), $\Delta S°$ (III → I) and $(dP/dT)_{III/I}$ were calculated as shown in Table III. The present value of $\Delta S°$ (III → I) is $+5.0$ J K^{-1} while the earlier value is 0 J K^{-1} (*3*). However, since the $\Delta V°$ for the transition is very large, the calculated phase boundary itself is in good agreement with the measured one. This suggests that it is difficult to constrain the ΔS from the phase equilibrium study alone for the III/I transition.

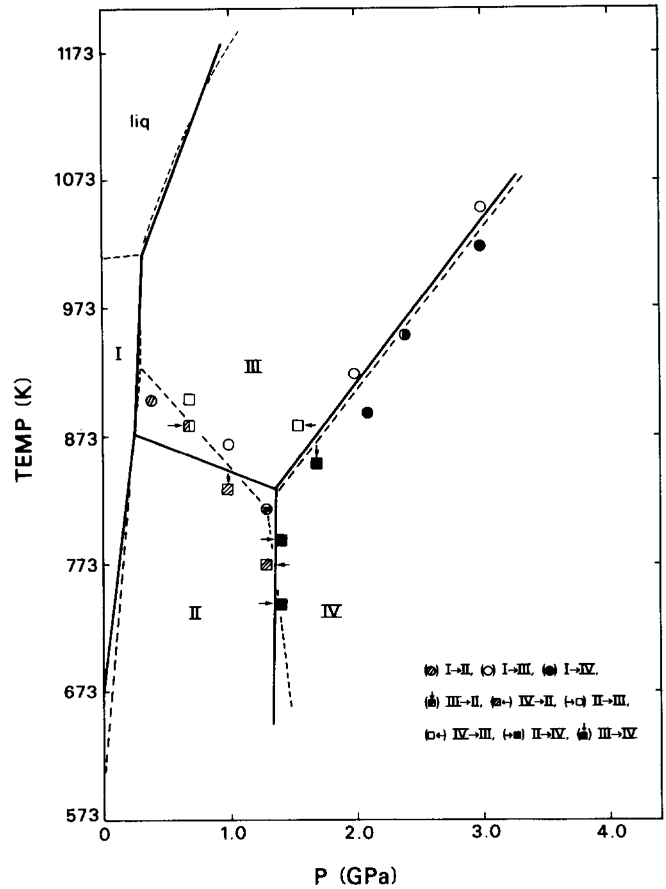

FIG. 1. The phase diagram of Li_2WO_4. Dashed lines show phase boundaries from Yamaoka *et al.* (*2*), and Pistorius (*3*). Solid lines show phase boundaries calculated in the present work. Experimental runs from Yamaoka *et al.* (*2*) (only the runs near phase boundaries are shown).

Our triple point (I/II/III) is 875 K, 0.25 GPa. The phase boundary of I/II based on this point intersects the T axis at 667 K indicating that the Li_2WO_4I is not a stable phase at room temperature and atmospheric pressure. This is consistent with the phase equilibrium study by Pistorius (3).

From the earlier value of $(dP/dT)_{I/liq}$ and melting point of Li_2WO_4I (1013 K) (3) and the present heat of fusion for Li_2WO_4I, the $\Delta V°$ (I → liq) and $\Delta S°$ (I → liq) were calculated as shown in Table III. For the transition of III/liq, the thermochemical data are easily obtained from the data on the transition of I/liq and I/III. For instance,

$$\Delta S° (\text{III} \rightarrow \text{liq}) = \Delta S° (\text{III} \rightarrow \text{I}) + \Delta S° (\text{I} \rightarrow \text{liq}). \quad (4)$$

The results thus obtained are listed in Table III. Pistorius also reported thermochemical data for the transition of I/liq and III/liq calculated from his experimental values of $(dP/dT)_{I/liq}$, $(dP/dT)_{III/liq}$, and ΔS (I → III) (3). Considering the experimental errors, the agreement between our and his values is fairly good (Table III).

Comparing the overall phase diagrams, the present one based on thermochemical data is in good agreement with the previous one based on high-presure experiments except for the II/III phase boundary. More careful phase equilibrium experiments or direct measurements of the entropy change would be needed to locate the II/III phase boundary.

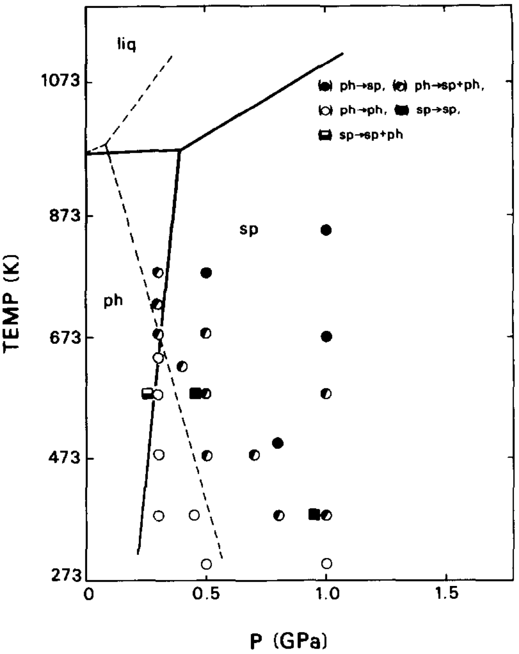

FIG. 2. The phase diagram of Li_2MoO_4. Dashed lines show phase boundaries from Liebertz and Rooymans (1). Solid lines show phase boundaries calculated in the present work. Experimental runs from Liebertz and Rooymans (1).

Phase Diagram of Li_2MoO_4

Almost all of the runs of the phase study of Liebertz and Rooymans (1) are in one direction, namely from phenacite to spinel. Moreover they found trace amount of spinel phase in the samples within their assumed phenacite region, though they explained this by an inevitable lack of homogeneity in pressure. It is, therefore, difficult to get a reliable point of equilibrium between Li_2MoO_4(ph) and Li_2MoO_4(sp). Only one reversal experiment was done at 580 K and 0.3 GPa, where they obtained a mixture of phenacite and spinel phases starting from spinel prepared at 673 K and 2 GPa (1). Taking the midpoint between this and other run (680 K, 0.3 GPa) where the phenacite to spinel transition was confirmed, we chose an equilibrium point of 630 K, 0.3 GPa. The calculated $\Delta S°$ and dP/dT were determined are shown in Table III. The present $\Delta S°$ (sp → ph) is slightly positive while that reported by Liebertz and Rooymans is negative (-8.4 J K^{-1}) (1). The transition curve in the present work shows, therefore, a slightly positive value of dP/dT (see Fig. 2). Considering the possibility of low transformation rates in the lower temperature region, it seems impossible to get an unambiguous phase boundary from the experimental runs alone. The thermochemical data may help constrain this boundary, and argue for a small positive dP/dT.

Since the volume change of the ph/liq transition is not known, it was assumed to be the same as that of the Li_2WO_4I/liq transition (0.45 cc/mole). Using this value and the melting point of Li_2MoO_4(ph) (978 K) (*1*), $\Delta S°$ (ph → liq) and $(dP/dT)_{ph/liq}$ were calculated (see Table III). By the same method as for Li_2WO_4III/liq, thermochemical data on the transition of Li_2MoO_4 sp/liq were obtained (Table III).

We conclude that there is a serious discrepancy between the present and previous phase diagram. These differences may be related to slow reaction rates and lack of reversals at lower temperatures. Carefully reversed high-pressure experiments at higher temperature would help resolve these problems.

Stability Relation among Li_2MoO_4(ph), Li_2MoO_4(sp), and Melt

Goldschmidt claimed Li_2MoO_4 changes to a spinel form at elevated temperature and atmospheric pressure (*16*). Liebertz and Rooymans showed, however, that it undergoes no transition up to the melting point (*1*). The present study also contradicts Goldschmidt's prediction. In particular, $\Delta S°$ (ph → sp) is negative, so the spinel cannot be a stable high-temperature phase. However, as described above, the spinel phase can be prepared at atmospheric pressure by quenching the melt. Also, the solidification peak in the DTA diagram of Li_2MoO_4 is very broad and shows evidence of large supercooling. These facts seem to indicate that the phenacite phase generally crystallizes from the melt by first passing through the metastable spinel phase. This may suggest that the melt may have some structural features, perhaps Li in higher than fourfold coordination, making it easier to nucleate spinel from it. The volume of fusion of Li_2WO_4 is quite small, suggesting that little expansion occurs on melting the phenacite phase. The expansion expected on disordering the crystal may be partly compensated by increasing local coordination. This point needs further study. However, we stress that our data indicate that the spinel is not a stable phase at atmospheric pressure.

Discussion of Energetics

Figure 3 shows the energetics of various

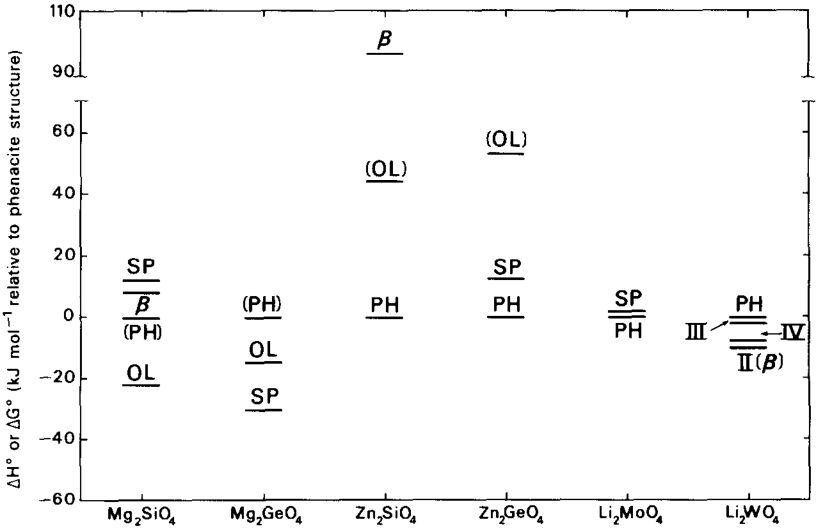

FIG. 3. Energetics relative to the phenacite structure for selected compounds.

partly octahedrally coordinated polymorphs relative to the all-tetrahedral phenacite structure for Li_2MoO_4 and Li_2WO_4 and for the silicates and germanates of Zn and Mg. Compared to the wide range of energies for the 2–4 charge type materials $(M_2^{2+}T^{4+}O_4)$, the 1–6 materials $(Li_2^{+}T^{6+}O_4)$ show a strikingly small range of energetics, with all polymorphs within 10 kJ in enthalpy, and several within 2 kJ. For Li_2MoO_4 the phenacite is energetically slightly more stable than the spinel; for Li_2WO_4 all polymorphs with Li in octahedral coordination are energetically more stable, but apparently of lower entropy (as discussed above) than the phenacite structure. The enthalpy to transform the phenacite structure to the energetically most stable polymorph with octahedrally coordinated M^+ or M^{2+} is -21.8 kJ for Mg_2SiO_4, -29 kJ for Mg_2GeO_4, 43.9 kJ for Zn_2SiO_4, 12.0 kJ for Zn_2GeO_4, -9.9 kJ for Li_2WO_4, and $+1.6$ kJ for Li_2MoO_4. The differences between Mg_2SiO_4 and Mg_2GeO_4, Zn_2SiO_4 and Zn_2GeO_4, and Li_2WO_4 and Li_2MoO_4 emphasize that the cation remaining in tetrahedral coordination (Si, Ge, Mo, or W) influences both the energetics of the phase transition and the structure of the phases formed (olivine, spinel, modified spinel (β) or others). No simple relation is apparent between the enthalpy of transition and some general atomic property describing octahedral versus tetrahedral site preference, such as ionic radius (*17*), octahedral site preference energy in the spinel structure (*18*), Pauling electronegativity (*19*) or Phillips ionicity (*20*). Rather, the energetics appear to be determined by detailed structural factors in the solid state, which dictate a delicate balance of enthalpy, entropy, and volume contributions to the free energy.

Acknowledgments

One of the authors (E.T.) thanks Mrs. Kobayashi and Mr. Yajima of NIRIM for the chemical analysis and Mr. C. Skiba and Dr. D. Ziegler of ASU for useful suggestions on the calorimetric measurement. This work was supported by NSF Grant DMR 8106027.

References

1. J. Liebertz and C. J. M. Rooymans, *Solid State Commun.* **5**, 405 (1967).
2. S. Yamaoka, O. Fukunaga, T. Ono, E. Iizuka, and S. Asami, *J. Solid State Chem.* **6**, 280 (1973).
3. C. W. F. T. Pistorius, *J. Solid State Chem.* **13**, 325 (1975).
4. K. Waltersson, P. E. Werner, and K. A. Wilhelmi, *Cryst. Struct. Commun.* **6**, 231 (1977).
5. H. Horiuchi, N. Morimoto, and S. Yamaoka, *J. Solid State Chem.* **30**, 129 (1979).
6. K. Waltersson, P. E. Werner, and K. A. Wilhelmi, *Cryst. Struct. Commun.* **6**, 225 (1977).
7. H. Horiuchi, N. Morimoto, and S. Yamaoka, *J. Solid State Chem.* **33**, 115 (1980).
8. K. A. Wilhelmi, K. Waltersson, and P. Löfgren, *Cryst. Struct. Commun.* **6**, 219 (1977).
9. A. Navrotsky, J. C. Jamieson, and O. J. Kleppa, *Science* **158**, 388 (1977).
10. Joint Committee on Powder Diffraction Standards, No. 24-664 (1974).
11. Japan Industrial Standard K0102 (1971).
12. G. T. Furukawa, T. B. Douglas, R. E. McCoskey, and D. C. Ginnings, *J. Res. NBS* **57**, 2694 (1956).
13. K. K. Kelley, *U.S. Bur. Mines Bull.* **584** (1960).
14. Joint Committee on Powder Diffraction Standards, No. 12-760 (1962).
15. Joint Committee on Powder Diffraction Standards, No. 12-763 (1962).
16. V. M. Goldschmidt, *Skr. Akad. Oslo* **2**, 107 (1926).
17. R. D. Shannon and C. T. Prewitt, *Acta Crystallogr. Sect. B* **25**, 925 (1969).
18. H. O'Neill and A. Navrotsky, *Am. Mineral.* **69**, 733 (1984).
19. L. Pauling, "The Nature of the Chemical Bond," Cornell Univ. Press, Ithaca, N.Y., 1960.
20. J. C. Phillips, *Rev. Modern Phys.* **42**, 317 (1970).
21. M. Akaogi, N. L. Ross, P. McMillan, and A. Navrotsky, *Am. Mineral.* **69**, 499 (1984).
22. A. Navrotsky, *Calphad* **4**, 255 (1980).